 DOI: 10.1002/masy.200650122

Novel Copolymers as Dispersants/Intercalants/ Exfoliants for Polypropylene-Clay Nanocomposites

Graeme Moad,[*1] *Katherine Dean,*[2] *Lex Edmond,*[2] *Natalia Kukaleva,*[2] *Guoxin Li,*[1] *Roshan T A Mayadunne,*[1] *Rudolf Pfaendner,*[3] *Armin Schneider,*[4] *George Simon,*[2] *Hendrik Wermter*[3]

Summary: The use of various copolymers as dispersants/intercalants/exfoliants in polypropylene (PP)-clay nanocomposites based on unmodified montmorillonite clays (NaMMT) has been explored. The primary objective of this research has been to find dispersants that allow PP nanocomposites to be formed by direct melt mixing, that are effective with unmodified clays and that comprise only a minor component of the overall composition both with respect to both clay and PP. Two classes of dispersants were investigated: PEO-based nonionic surfactants and amphiphilic copolymers based on a long chain (meth)acrylate (e.g. octadecyl acrylate) and a more polar comonomer (e.g. maleic anhydride, N-vinylpyrrolidone, methyl methacrylate). The state of dispersion achieved and the properties of the derived nanocomposites were found to depend strongly on both on the level of dispersant and its overall composition but interestingly properties are not particularly dependent on the dispersant architecture (i.e. whether statistical, gradient or block copolymer). The nanocomposites possess a tensile modulus up to 40% greater that the precursor PP while elongation at break and impact strength are significantly improved over ''clay alone'' composites and reference organoclay-based nanocomposites. Also notable are significantly better thermal and thermo-oxidative stability as compared to both PP and ''clay alone'' composites. For optimal properties, it is both necessary and desirable that the surfactant should only be a minor constituent (20–50 wt-%) of the composition with respect to clay.

Introduction

The first reports of explicitly designed polymer-clay nanocomposites appeared in the early 90's.[1,2] Since that time the nanocomposite literature has expanded rapidly. The attractions of nanocomposites from an applications viewpoint are that they can possess better tensile properties (higher elastic modulus and tensile strength), improved barrier properties (lower liquid and gas permeability), higher heat distortion temperature, and display greater flame retardancy. There is now a substantial literature on clay-based nanocomposites and most reviews cover, in part, polyolefin nanocomposites.[3–5]

Clay particles consist of agglomerated tactoids (see Figure 1). It is generally believed that these particles must be broken down to individual tactoids and ideally further exfoliated to individual clay layers which are dispersed within the polyolefin matrix to achieve optimal property enhancement. Factors such as the aspect ratio of

Cooperative Research Centre for Polymers

[1] CSIRO Molecular and Health Technologies, Bag 10 Clayton South, Victoria 3169, Australia
[2] SPME, Monash University, Clayton, Victoria 3168, Australia
[3] Ciba Specialty Chemicals Inc., Lampertheim, Germany
[4] Ciba Specialty Chemicals Inc., Basel, Switzerland
E-mail: graeme.moad@csiro.au

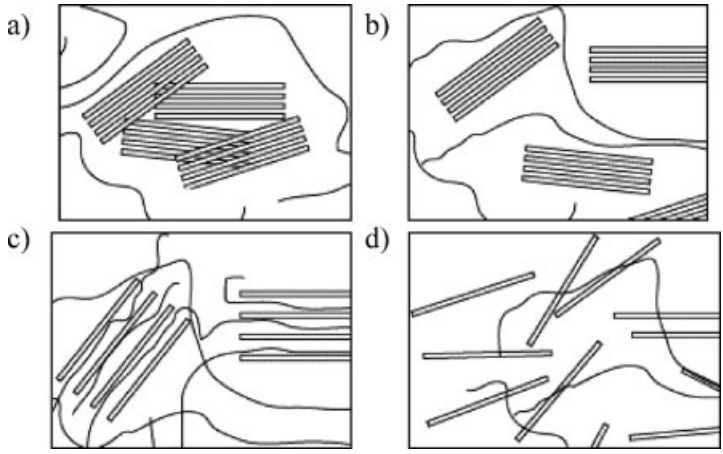

Figure 1.
Schematic representation of four clay composite structures which consist of: a) agglomerated tactoids, b) individual tactoids, c) intercalated tactoids, d) exfoliated clay layers.

the clay and degree of orientation of the clay particles in the final structure are also thought to be important in determining properties.[6]

Although there are reports that exfoliated nanocomposites may be prepared directly from polyolefins and unmodified clays by high shear mixing, most work on polyolefin nanocomposites has made use of organophilic clays.[7–9] These organophilic clays are typically derived from purified sodium montmorillonite by cation exchange with a long chain amine or a quaternary ammonium salt which may then comprise up to 40 wt-% of the clay. Some problems with these systems have been identified. Particularly pertinent is the instability of ammonium salts at temperatures encountered in melt processing of PP. PP nanocomposites also typically contain an additional 'compatibilizing agent'; most often this is a maleic anhydride grafted PP (MAH-graft-PP). Thus, PP nanocomposites described in the literature typically contain between 5–25% of MAH-*graft*-PP. In some cases, so-called PP nanocomposites comprise entirely modified PP.

Our efforts have been directed to finding a solution to these issues by designing intercalants/dispersants that are effective with unmodified clays at low levels (<20% with respect to clay), can be combined with commercial polypropylene and clay in a conventional melt mixing process, and do not require the use of additional compatibilizers.[10] In recent publications[11,12] we have reported on the use of poly(ethylene oxide) (PEO)-based nonionic surfactants as dispersants/intercalants/exfoliants in this context. In this paper, we summarize this work and report on the use of amphiphilic copolymers based on long chain acrylates in a similar context.

Experimental Part

Gel permeation chromatography (GPC) was performed on a Waters Associates liquid chromatograph equipped with differential refractometer and $3 \times$ Mixed C and 1 mixed E PLgel column (each 7.5 mm $\times$ 30 mm) from Polymer Laboratories. Tetrahydrofuran (flow rate of 1.0 mL/min) was used as eluent at $22 \pm 2\,^{\circ}C$ and the columns were calibrated with narrow polydispersity polystyrene standards (Polymer Laboratories).

The PP used was Moplen® HP400N (Basell, Australia) [MFR (230 °C/2.16 kg, ISO 1133) 11 g/10 min]. The montmorillonite clay used was Cloisite Na+® (Southern Clay Products, Inc.). Stabilizer Irganox® B225 (Ciba Specialty Chemicals) was

added during melt compounding to all compositions (0.2 wt-% of PP). Nanocomposites were prepared by melt mixing in a twin screw extruder by first forming a masterbatch comprising 10–70 wt-% clay plus other components which was then melt-blended with further PP to form a nanocomposite of the required clay content. A reference nanocomposite was prepared by a similar process using 5 wt-% of organophilic clay, Cloisite® 20A (modified with dimethyl, di(hydrogenatedtallow)ammonium chloride) obtained from Southern Clay Products, Inc., USA and with 7.5 wt-% Polybond® 3200, a MAH-*graft*-PP [from datasheet: MAH level 1 wt.-%, density 0.91 g/mL, MFR (190 °C/2.16 kg) 115 g/10 min, ASTM D1238] supplied by Crompton, Australia.

The linear PEO-based surfactants **1a–d** were obtained from Aldrich Chemical Co. The low molecular weight PE-*block*-PEO (**1e**), the branched polymer (**2**), the sorbitan derivative (**3**) and the gemini surfactants (**4** and **5**) were supplied by Ciba Specialty Chemicals. Block lengths were determined by NMR analysis as described elsewhere.[12,13]

Monomers, octadecyl acrylate (ODA), *N*-vinyl pyrrolidone (NVP), and maleic anhydride (MAH), were obtained from Aldrich. Copolymers [poly(ODA-*grad*-MAH) **6** and poly(ODA-*grad*-NVP) **7**] were synthesized by RAFT polymerization.[14]

Poly(octadecyl acrylate-*grad*-*N*-vinyl pyrrolidone) (7)

A solution of ODA (200.0 g, 616 mmol), NVP (17.1 g, 154 mmol), S-butyl S-(1-phenylethyl) trithiocarbonate (3.0g, 10.9 mmol), AIBN (178 mg, 1.09 mmol) in 200 mL of dry toluene was degassed by purging with argon for 3 h. Polymerization was carried out at 60 °C with stirring under argon for 21 h. The solution was then poured into 2.5 L of vigorously stirred acetone. The polymer was collected by filtration and vacuum-dried to leave a yellow solid: conversion: 94%; [ODA]:[NVP] 3:1, $\overline{M}_n$(NMR) 19300, $\overline{M}_n$(GPC, polystyrene equivalents) 16200, $\overline{M}_w/\overline{M}_n$ 1.23.

Poly(octadecyl acrylate-*grad*-maleic anhydride) (6)

A solution of ODA (450.0 g, 1387 mmol), MAH (45.3 g, 462 mmol), S-dodecyl S-(1-phenylethyl) trithiocarbonate (9.5g, 24.8 mmol), AIBN (0.81 g, 4.9 mmol) in 1 L of dry tetrahydrofuran was degassed by purging with argon for 3 h. Polymerization was carried out at 60 °C with stirring under argon for 49 h. The solution was concentrated to ~550 mL then poured into 2.5 L of vigorously stirred acetone. The polymer was collected by filtration and vacuum-dried to leave a yellow solid: conversion: 93%; [ODA]:[MAH] 3:1 and $\overline{M}_n$(NMR) 19300, $\overline{M}_n$(GPC, polystyrene equivalents) 6300, $\overline{M}_w/\overline{M}_n$ 1.3.

Processing was carried out with a Japan Steel Works 30 mm diameter twin screw extruder of L/D 42 (JSW TEX 30) that comprised ten temperature controlled barrel sections each with L/D of 3.5 (set at 170 °C for masterbatch preparation and 200 °C for the final extrusion step) three unheated sampling zones with L/D 1.167, and a cooled feed block with L/D 3.5. Materials were fed into the extruder via a JSW TTF20 gravimetric feeder (Feed 1) or a K-Tron KQX gravimetric feeder (Feed 2). The JSW TEX 30 was operated in corotating (intermeshing, self wiping) mode with a throughput of 10 kg/hr and a screw speed of 200 rpm. Vacuum venting was applied to the final barrel section. The extrudate was cooled in a water filled strand bath and pelletized.

Injection molding of the extruded samples into standard dumbbells was performed with a Cincinnati Milacron Sentry Vista injection molder (Model VS55-2.27) with a 28 mm diameter feed screw of compression ratio 2.0. The extruder was operated at 220 rpm. The barrel temperatures for the three heated zones were set at 215, 225, and 220 °C, the nozzle temperature at 235 °C and the mold temperature at 36 °C. The pack time was set at 7 s (pressure

35 bar), the hold time at 10s (pressure 50 bar, 55 bar, 45 bar) and the cool time at 30 s.

Wide Angle X-Ray Scattering analysis was conducted using a Rigaku-Geigerflex X-ray diffractometer scanning with Ni filtered CuKα radiation. Scans were taken from 1–30° at a speed of 1°/min and a step size of 0.05°.

For scanning electron microscopy (SEM), cryofracture surfaces taken from central section of tensile bars perpendicular to the flow direction were studied using a FEI QUANTA 200 environmental scanning electron microscope (ESEM^{TM}) operated in a Low Vacuum mode at an accelerating voltage of 10 or 20 kV. The pressure in the specimen chamber was set at 0.5 Torr; water vapor was used as an environment.

For transmission electron microscopy (TEM) ultra-thin sections (50–90 nm) were prepared at −140 °C with a Reichert FSC ultracut S ultramicrotome using a diamond knife. Samples were taken from central section of tensile bars perpendicular to the flow direction. The sections were pressed onto 300 mesh copper grids and the TEM measurements of these sections were carried out on a Phillips CM20 transmission electron microscope operating at 120 kV.

Tensile testing was performed according to ISO 527 using an Instron 5500R material tensile tester equipped with a 5 kN load cell and Instron Merlin software Version 22055 (2001). Tensile bars (HP400N) had dimensions 150 mm × 9.86 mm × 3.35 mm with a gauge length of 50 mm. The testing temperature was 23 ± 2 °C. The samples were conditioned in this environment for a minimum 88 h prior to testing. Modulus and tensile strength measurements were determined with a crosshead speed of 1 mm min^{-1}. A 50 mm static extensometer (model 2630–111) was employed and the modulus was measured between 0.05 and 0.25% strain. Values of elongation at break were determined without the extensometer and a crosshead speed of 50 mm min^{-1}. The results were averaged over 6–10 samples.

Differential scanning calorimetry (DSC) was carried out with at Mettler DSC821 equipped with a T50 801 sample robot. DSC was conducted on samples (~5 mg) taken from tensile bars in sealed aluminium sample pans. Samples were heated from 25–225 °C at 10°/min, cooled 225–25 °C at 10°/min, then heated again from 25–225 °C at 10°/min.

Thermogravimetric analysis (TGA) was carried out with a Mettler thermobalance T6A/SDTA851 equipped with a T50 801 sample robot. Cryoground samples (~10 mg) were heated from 50 to 500 °C at 10 °C/min in alumina crucibles in an air or nitrogen atmosphere as indicated.

Copolymer Dispersants

PEO-based nonionic surfactants studied included linear polyethylene-*block*-PEO (**1a–e**) (PE-*block*-PEO), branched structures (**2**) sorbitan derivatives (**3**) and gemini surfactants (**4**, **5**). The values for chain lengths indicated are average values. Details of the characterization of these compounds are reported elsewhere.[12] Amongst the linear surfactants **1**, the compound was **1**d with a relatively short PEO-block and a ~C_{40} alkyl chain proved most effective. [12]

A series of copolymers all based on long chain acrylates or methacrylates but of differing composition, molecular weight and architecture (homopolymers, statistical copolymers, gradient copolymers, block copolymers and) were prepared.[10] Copolymers based on dodecyl acrylate (DA) and octadecyl acrylate (ODA) were similarly effective. Copolymers based on BA were poorer dispersants. ODA copolymers, being solids (mp ~60 °C), were easier to handle and were more readily purified than DA copolymers. The choice of polar monomer did not appear crucial to the properties of the copolymer as a dispersant in the present application. While most of the polymers examined offered beneficial properties, some preferred copolymers contained octadecyl acrylate (ODA) or methacrylate (ODMA) as the long chain acrylate and MMA, NVP or MAH as a

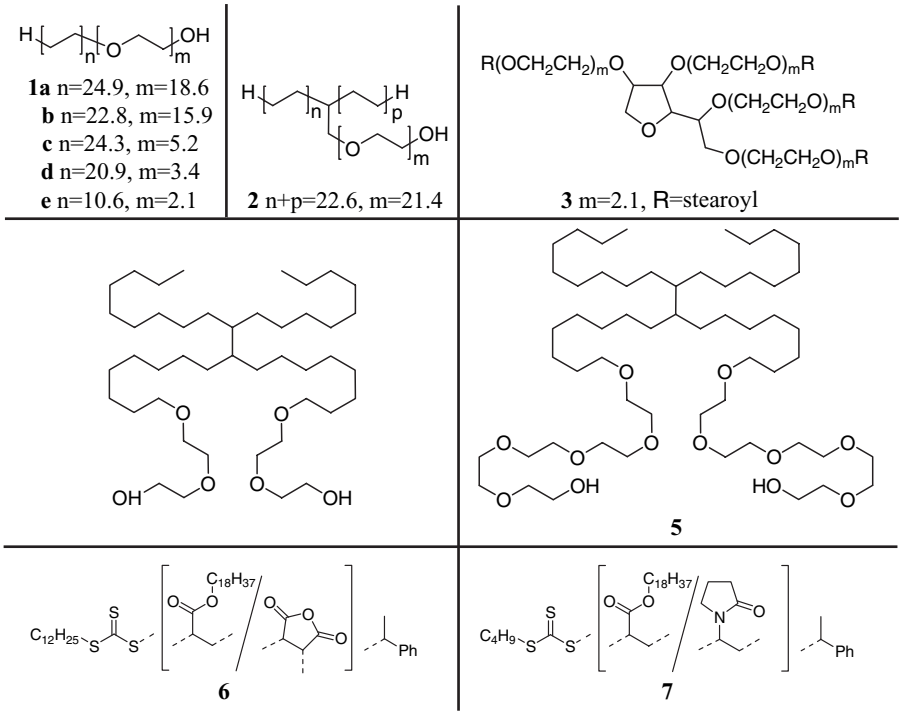

polar monomer. With the relatively non-polar poly(MMA-*co*-ODMA) it was found necessary to pre-blend the clay and additive to achieve optimal properties.

Gradient copolymers, *e.g.* poly(ODA-*grad*-MAH) **6** or poly(ODA-*grad*-NVP) **7,** were prepared by RAFT polymerization[15] with S-dodecyl S′-phenylethyl trithiocarbonate or S-butyl S′-phenylethyl trithiocarbonate). These copolymers provided slightly better properties than statistical copolymers of similar overall composition prepared by conventional radical polymerization. The difference is attributed to a greater uniformity of composition for the copolymer prepared by living radical polymerization. An additional factor is that these copolymers had a narrow molecular weight distribution ($\overline{M}_w/\overline{M}_n \leq 1.2$) whereas those prepared by conventional radical copolymerization had (depending on the comonomer) a relatively broad molecular weights distribution ($\overline{M}_w/\overline{M}_n$ in range 2–8). Attempts were made to control molecular weight and dispersity using conventional chain transfer agents or by controlled addition of initiator. For some systems A-B diblocks of nominally similar overall composition were also prepared either by RAFT[15] or in some cases by ATRP or NMP. The block copolymer dispersants did not offer any advantage over statistical or gradient copolymers.

Characterization of Nanocomposites

WAXS/SEM/TEM

The most used methods for characterizing the state of the clay particles in nanocomposites are wide angle X-ray scattering (WAXS) and transmission electron microscopy (TEM). It should be noted that fully exfoliated structures are not generally observed for predominantly PP nanocomposites even with conventional organoclays. The WAXS patterns of PP nanocomposites containing 5 wt.-% Cloisite Na^+ show that the peak (d-spacing $d_{001} \sim 10$ Å, $2\theta \sim 8.9°$) associated with the unmodified Cloisite Na^+ is substantially

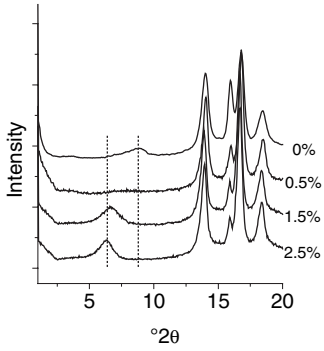

Figure 2.
Wide angle X-ray scattering patterns for polypropylene (HP400N) nanocomposites with 5 wt-% Cloisite Na+ (a) without dispersant or with (b) 0.5 wt-% **1d**; (c) 1.5 wt-% **1d**; (d) 2.5 wt-% **1d** as dispersant. [12]

reduced in intensity by addition of 0.5% PE-*block*-PEO surfactant **1d** (Figure 2). A peak at higher d-spacing ($d_{001} \sim 14$ Å, $2\theta \sim 6.3^\circ$) appears on addition of larger amounts of the surfactant. Analogous behavior was seen with the other additives. The branched surfactants and those with longer PEO blocks provided slightly greater expansion of the clay.[12] However, both the non-ionic surfactants and the acrylic copolymers provide only a small expansion of the clay ($d_{001} < 20$ Å, $2\theta > 4.5^\circ$). No correlation was observed between the degree of expansion observed and tensile or other properties of the nanocomposite.

The position of the d_{001} peak does not vary substantially with clay/additive concentration but appears disproportionately weak with low additive (Figure 2) and low clay levels.[12] The absence of peaks in the WAXS patterns clearly should not be taken as evidence for exfoliation.[16,17]

WAXS patterns show that the PP (Moplen HP400N) as molded contains a significant β-crystalline fraction. This fraction is enhanced by addition of Cloisite Na+ and increases with clay level.[12] The β-crystalline fraction remains significant though slightly reduced in the nanocomposites incorporating the PEO based (e.g. Figure 2) or copolymer dispersants. By contrast, and consistent with reports in the literature, for nanocomposites prepared with the organoclay Cloisite 20A with MAH-*graft*-PP (Polybond 3200) the β-crystallinity is largely suppressed.[18,19] Optical microscopy show a dramatic reduction in crystallite size for all nanocomposites vs PP.

Low resolution ESEM images (Figure 3) show that Cloisite Na+ alone composites contain occasional large clay particles (>100 μ). However, most of the particles are ~10–100 μ. There are very few particles <2 μ. For nanocomposites with 1 wt-% **1c** or **d**, the occasional large clay particles remain, there are fewer particles in the size range 10–100 μ and most of the particles are <2 μ. For nanocomposites with 1 wt-% **1a** or **b** there appear less small particles <2 μ. For nanocomposites with 1 wt-% copolymer most of the particles are <2 μ. Note that the scale of these images is such that small particles like tactoids and individual clay layers such as those seen in the TEM images (*e.g.* Figure 4) will not be visible.

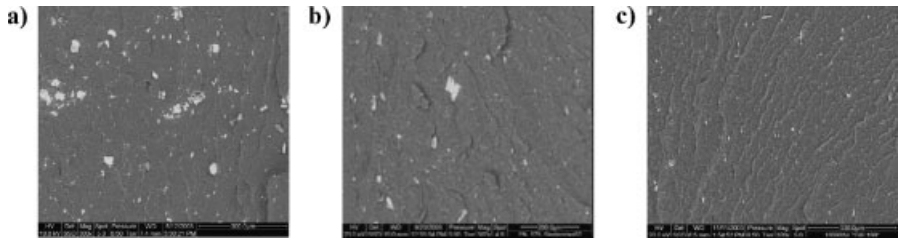

Figure 3.
Lower resolution SEM images of fracture surfaces for polypropylene (HP400N) nanocomposites with (a) 5 wt-% Cloisite Na+ alone, (b) 5 wt-% Cloisite Na+ and 1% nonionic surfactant **1d**, (c) 5 wt-% Cloisite Na+ and 1 wt-% copolymer poly(ODA-*grad*-MAH) **6**.

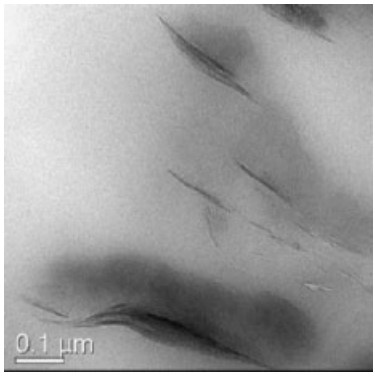

Figure 4.
TEM images of polypropylene (HP400N) nanocomposite containing 5 wt-% Cloisite Na+ and 1 wt-% copolymer 1 wt-% poly(ODA-*grad*-MAH) **6**.

The TEM images (Figure 4) also indicate that most agglomerates (other than the very large ones) have been largely broken down to tactoids consisting of a few clay layers. There are also occasional single clay layers. There is partial exfoliation.

The visual appearance of nanocomposites containing 5 wt-% Cloisite Na+ and 1% acrylic copolymer is similar to those of 'benchmark' systems prepared with organoclay (Cloisite 20A) with 15 wt-% poly(MAH)-*graft*-PP as compatibilizer. Very similar results were obtained using a range of copolymers.

Mechanical Properties

Conventional organoclay nanocomposites show improvements in modulus and tensile strength and a marked decrease in elongation at break with respect to PP. The systems based on unmodified clay (Cloisite Na^+) and our dispersants also show significant improvements in modulus, of 20–30%, and a significantly more ductile than reference nanocomposites based on an organophilic clay (Cloisite 20A) with PP-*graft*-MAH (Table 1).

It is of interest that the additives (**1d**, **6**) have the effect of simultaneously improving both the modulus and the elongation at break. The improvement in properties for the Cloisite Na^+ based nanocomposites is in line with the extent of exfoliation is observed by microscopy and improvements thermal and thermooxidative stability follow the same trend. Differences in crystallinity (*vide infra*) may in part account for the greater ductility and slightly lower modulus of the systems based on Cloisite Na^+ vs the organoclay based systems. The β-crystalline form of PP is known to be more ductile.

Thermal Analysis

DSC analysis showed that the % crystallinity and melting temperature of samples taken from the injection molded bars of PP, PP with Cloisite Na^+ and PP with Cloisite Na^+ and copolymer are very similar. This finding is consistent with the WAXS spectra.

It has been reported that organoclay-based PP nanocomposites with 15 wt-% MAH-*graft*-PP with respect to PP have

Table 1.
Summary of Tensile Properties for Polypropylene Samples

Material	Elongation at break		Elastic modulus	
	actual%	rel. PP %	actual (MPa)	rel. PP
PP	(~1000)	100	1500	1
Cloisite Na[a)]	20–40	2–4	~1700	1.2
" + **1d**[b)]	30–120	3–12	1700–1800	1.2
" + **6**[c)]	100–300	10–30	1800–2000	1.2–1.3
" + **6** + PB[d)]	60	6	2000	1.3
Cloisite 20A + PB[e)]	40	4	2200	1.4

[a)] 5 wt-% Cloiste Na.
[b)] 5 wt-% Cloiste Na and 1 wt-% PEO-*block*-PE (**1d**.).
[c)] 5 wt-% Cloiste Na and 1 wt-% poly(ODA-*grad*-MAH) (**6**).
[d)] 5 wt-% Cloiste Na, 1 wt-% poly(ODA-*grad*-MAH) (**6**) and 7.5 wt-% PP-*graft*-MAH (Polybond 3200).
[e)] 5 wt-% Cloiste 20A and 7.5 wt-% PP-*graft*-MAH (Polybond 3200).

Table 2.
Differential Scanning Calorimetry Melting/Crystallization Data for Polypropylene Samples Heated/Cooled at 10 °C min^{-1}

Material/Parameter	1st melting			Crystallization			2nd melting		
	%Cr	T_m onset °C	T_m °C	%Cr	T_{cr} onset °C	T_{cr} °C	%Cr	T_m onset °C	T_m °C
PP[a]	41.8	147.6	166.1	44.5	120.5	116.1	45.6	154.4	161.7
+clay[b]	40.5	151.8	165.4	45.4	122.4	120.4	46.0	155.8	162.5
+**1d**[c]	40.5	160.2	166.8	45.5	121.3	117.4	45.8	154.2	162.7
+**7**[d]	42.8	154.8	166.5	45.1	120.2	115.2	45.8	153.9	161.3
+**6**[e]	41.4	156.4	167.7	46.1	119.9	115.3	45.8	153.4	162.0

[a] Polypropylene (PP, Moplen HP400N) processed with 0.2 wt-% B225 stabilizer.
[b] with 5 wt-% Cloiste Na.
[c] with 5 wt-% Cloiste Na and 1 wt-% PEO-*block*-PE (**1d**).
[d] with 5 wt-% Cloisite Na^+ and 1 wt-% poly(ODA-*grad*-MAH) (**6**).
[e] with 5 wt-% Cloisite Na^+ and 1 wt-% poly(ODA-*grad*-NVP) (**7**).

improved thermal and thermooxidative stability as measured by thermogravimetric analysis (TGA).[20]

TGA analysis shows that the thermooxidative stability of nanocomposites prepared with 5 wt-% unmodified clay and 1 wt-% copolymer is significantly improved with respect to PP or PP with the clay alone (Table 3, Figure 5a). The improvement is most marked (~40 °C) for the samples with 1 wt-% of the acrylic copolymer additives **6** or **7**. The thermooxidative stability of these materials is not as great as that of a reference organoclay-based nanocomposite prepared with 5 wt-% Cloiste 20A and 7.5 wt-% PP-graft-MAH (Table 3). We can note that PP-graft-MAH by itself acts as a stabilizer for PP under air (Table 3) and with Cloisiste Na^+ appears as effective as copolymers **6** or **7**.[20]

The thermal stability under nitrogen is also improved over PP for the nanocomposite samples with copolymer **6** or **7** (Table 3, Figure 5b). The addition of Cloisite Na or PP-graft-MAH by themselves have no substantial effect on the

Table 3.
Mass Loss Data for Polypropylene Samples Heated at 10 °C min^{-1}

Sample	air				nitrogen			
	T_{10} °C	T_{max} °C	T_{90} °C	res. wt-%	T_{10} °C	T_{max} °C	T_{90} °C	res. wt-%
PP[a]	308	373	381	1.5	428	458	473	1.0
+Cloisite Na[b]	300	373	384	6.2	434	458	477	5.6
+Cloisite Na+**1d**[c]	319	391	401	5.5	435	455	472	6.2
+Cloisite Na+**6**[d]	328	407	416	6.2	447	469	483	6.0
+Cloisite Na+**7**[e]	330	402	411	5.8	444	470	485	5.5
+PB[f]	322	392	397	3.1	426	453	470	1.6
+Cloisite Na + PB[g]	337	413	418	6.1	436	456	474	5.9
+Cloisite 20A+PB[h]	338	436	437	5.4	434	443	447	4.3
+Cloisite 20A+PB+**6**[i]	350	417	433	6.4	446	465	477	5.3

[a] Polypropylene (PP, Moplen HP400N) processed with 0.2 wt-% B225 stabilizer.
[b] with 5 wt-% Cloisite Na^+.
[c] with 5 wt-% Cloisite Na^+ and 1 wt-% PE-*block*-PEO **1d**.
[d] with 5 wt-% Cloisite Na^+ and 1 wt-% poly(ODA-*grad*-MAH) (**6**).
[e] with5 wt-% Cloisite Na^+ and 1 wt-% poly(ODA-*grad*-NVP) (**7**).
[f] with 7.5 wt-% PP-*graft*-MAH (Polybond 3200).
[g] with 5 wt-% Cloisite Na^+ and 7.5 wt-% Polybond 3200.
[h] with 5 wt-% Cloiste 20A and 7.5 wt-% Polybond 3200.
[i] with 5 wt-% Cloiste 20A and 7.5 wt-% Polybond 3200 and 1 wt-% poly(ODA-*grad*-MAH) (**6**).

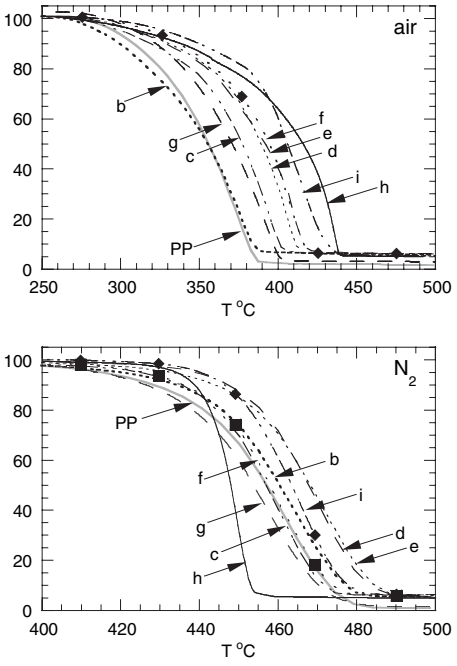

Figure 5.
TGA mass loss curves for heating rate 10 °C min^{-1} in air and under nitrogen for (a) polypropylene (PP, Moplen HP400N processed with 0.2 wt-% B225 stabilizer) (═══); (b) PP with 5 wt-% Cloisite Na^+ (·····); (c) PP with 5 wt-% Cloisite Na+ and 1 wt-% **1d** (- — -); (d) PP with 5 wt-% Cloisite Na^+ and 1 wt-% poly(ODA-*grad*-MAH) **6** (- - -); (e) PP with 5 wt-% Cloisite Na^+ and 1 wt-% poly(ODA-*grad*-NVP) **7** (– –); (f) PP with 7.5 wt-% PP-*graft*-MAH (— —); (g) PP with 5 wt-% Cloisite Na^+ and 7.5 wt-% PP-*graft*-MAH (- - -);(h) PP with 5 wt-% Cloiste 20A and 7.5 wt-% PP-*graft*-MAH (—); (i) PP with 5 wt-% Cloiste 20A and 7.5 wt-% PP-*graft*-MAH and 1 wt-% poly(ODA-*grad*-MAH) **6** (— — - -).

stability. The reference nanocomposite based on Cloisite 20A has comparatively poor thermal stability with a more sudden weight loss profile as reflected in a significantly lower T_{max} and lower T_{90} (Table 3). The thermal stability of the Cloisite 20A nanocomposite is also significantly enhanced by the addition of 1% copolymer **6**. It has been suggested that the anhydride functional copolymers (PP-graft-MAH) may sequester the amine byproducts derived from Hoffman elimination of the quaternary ammonium salt modifiers present in organoclays.

The 0.2 wt-% Irganox B225 which was added to all samples during processing imparts improvement to the thermal and thermooxidative stability of PP. The greater stability of PP observed in this study with reference to some literature reports may be attributed to the presence of this stabilizer.

The mechanism of stabilization by nanoparticulate fillers has been attributed in part[20] to the formation of a barrier which impedes both ingress of oxygen and evolution of volatiles. Consistent with this hypothesis we see an improvement in thermal stability according to the extent of exfoliation of the clay (additives **6** and **7** > additive **1d** > no additive).

Consistent with enhanced thermal stability, it was found that higher processing temperatures could be used both for producing the nanocomposite and in injection moulding with no adverse affect on PP properties. While nanocomposites were typically produced with extrusion temperatures of 200 °C and a throughput of 10 kg h^{-1}, several experiments showed that processing temperatures of 260 °C and throughput of 20 kg h^{-1} could be used without detriment to the MFI, tensile properties, color or state of clay dispersion and without formation of odorous by-products.

Conclusions

Polypropylene-clay nanocomposites can be prepared by direct melt mixing using unmodified montmorillonite clays and a copolymer additive added at a level of only 1 wt-% with respect to PP for 5 wt-% clay. The additives provide substantially improved clay dispersion and cause partial exfoliation. The nanocomposites have improved elastic modulus with respect to PP and are more ductile than conventional nanocomposites that are based on organoclays with PP-*graft*-MAH as additive. Also notable are better thermal and thermooxidative stability as compared to PP and ''clay alone'' composites.

[1] A. Okada, A. Usuki, *Mater. Sci. Eng. C-Biomimetic Mater. Sens. Syst.* **1995**, *3*, 109–15.
[2] E.P. Giannelis, *Advanced Materials* **1996**, *8*, 29–35.
[3] T. Pinnavaia, G. Beall, "*Polymer-Clay Nanocomposites*" John Wiley and Sons, Chichester 2000.
[4] H. Fischer, *Mater. Sci. Eng.* **2003**, *C23*, 763–72.
[5] S.S. Ray, M. Okamoto, *Prog. Polym. Sci.* **2003**, *28*, 1539–641.
[6] D.A. Brune, J. Bicerano, *Polymer* **2002**, *43*, 369–87.
[7] P. Reichert, H. Nitz, S. Klinke, R. Brandsch, R. Thomann, R. Mulhaupt, *Macromol. Mater. Eng.* **2000**, *275*, 8–17.
[8] G. Qian, T. Lan, *Plast. Eng.* **2003**, *67*, 707–28.
[9] A. Leuteritz, D. Pospiech, B. Kretzschmar, M. Willeke, D. Jehnichen, U. Jentzsch, K. Grundke, A. Janke, *Adv. Eng. Mater.* **2003**, *5*, 678–81.
[10] WO04113436 (2004), (Polymers Australia Pty. Limited, Australia). invs.: G. Moad, G.P. Simon, K.M. Dean, G. Li, R.T.A. Mayadunne, E. Rizzardo, R.A. Evans, H. Wermter, R. Pfaendner, *Chem. Abstr.* **2005**, *142*: 75401.
[11] G. Moad, K. Dean, L. Edmond, N. Kukaleva, G. Li, R.T.A. Mayadunne, R. Pfaendner, A. Schneider, G. Simon, H. Wermter, *World Polymer Congress, Macro 2004 Congress Proceedings*, **2004**, http://www.e-polymers.org/paris/data/L2702.pdf.
[12] G. Moad, K. Dean, L. Edmond, N. Kukaleva, G. Li, R.T.A. Mayadunne, R. Pfaendner, A. Schneider, G. Simon, H. Wermter, *Macromol. Mater. Eng.* **2005**, accepted for publication.
[13] A. Postma, A.R. Donovan, T.P. Davis, G. Li, G. Moad, R. Mulder, M. O'Shea, *Polymer* **2005**, submitted for publication.
[14] G. Moad, G. Li, E. Rizzardo, San H Thang, R. Pfaendner, H. Wermter, *Polym. Prepr. (Am. Chem. Soc., Div. Polym. Chem.)* **2005**, *46* (2), 376–7.
[15] G. Moad, E. Rizzardo, S.H. Thang, *Aust. J. Chem.* **2005**, *58*, 379–410.
[16] D.F. Eckel, M.P. Balogh, P.D. Fasulo, W.R. Rodgers, *J. Appl. Polym. Sci.* **2004**, *93*, 1110–7.
[17] A.B. Morgan, J.W. Gilman, *J. Appl. Polym. Sci.* **2003**, *87*, 1329–38.
[18] W. Zheng, X. Lu, C.L. Toh, T.H. Zheng, C. He, *J. Polym. Sci., Part B: Polym. Phys.* **2004**, *42*, 1810–6.
[19] T.S. Ellis, J.S. D'Angelo, *J. Appl. Polym. Sci.* **2003**, *90*, 1639–47.
[20] M. Zanetti, G. Camino, P. Reichert, R. Mulhaupt, *Macromol. Rapid Commun.* **2001**, *22*, 176–80.

